Materials Science and Technology, Volume 33, Issue 6, 2017, pp. 731-737
DOI:10.1080/02670836.2016.1243335

Reducing machining distortion in AA 6061 alloy through re-heating technique

Abdul Rafey Khan[a], Salman Nisar[a*], Aqueel Shah[a], Muhammad Ali Khan[b], Sohaib Zia Khan[b], Mohammed A. Sheikh[c]

[a,*]Department of Industrial and Manufacturing Engineering, [b] Department of Engineering Sciences,
PN Engineering College, National University of Sciences and Technology, PNS Jauhar, Karachi, 75350, Pakistan
[c]Manufacturing and Laser Processing Research Group, School of Mechanical, Aerospace and Civil Engineering,
The University of Manchester, Manchester, M60 1QD, UK

Abstract

Solution treated AA 6061 alloy contains residual stresses which cause unwanted deformation during the machining operation rendering the parts unacceptable for use. Usually for AA 6061 alloy, stress relieving is performed by re-heating the parts at 343 °C for 1 hr. This stress relieving is however accompanied by a considerable loss of material strength which subsequently reduces the functionality of the parts. This paper is based on an effort to evaluate the effectiveness of lower re-heating temperatures for stress relieving without significant loss of strength. Temperatures within the range of 200 °C to 343 °C were used and treated samples were tested for both the strength and machining distortion. The experimental results indicate 60% reduction in machining distortions with 21 % decrease in the strength.

Keywords: AA 6061 alloy; Machining distortion; Residual stresses; Re-heating; Strength loss; Electron microscopy; Secondary precipitates; Mechanical properties

*Corresponding author: Tel: +92(0)21 4850 3039
Email address: salman@pnec.nust.edu.pk

1. Introduction

Aluminum 6061 is a widely used alloy due to its light weight, high structural strength, good corrosion resistance, and weldability. Lee and Tang investigated the mechanical behavior of

6061 alloy in T6 temper at high strain rates and found it to possess considerable potential for thermo-mechanical forming without failure [1]. However, these favorable properties of T6 temper are attained via the solution treatment process which involves high temperature heating and rapid cooling of material resulting in residual stresses.

Dolan and Robinson have identified that the temperature gradient produced across the material during faster cooling is the main cause of residual stress. This gradient causes different areas of the material to cool differently resulting in non-uniform contraction which puts some areas in tension balanced by others in compression [2]. This state of residual stress presents serious problems during the machining operation wherein the stresses are released in the form of unwanted deformations making the part unacceptable for use. Dolan and Robinson proposed to use a combination of cooling rates during the solution treatment. For every material there is a critical range of temperature where a little time is sufficient to cause significant premature precipitation. The material should therefore be rapidly cooled within this range. Other than that a slower cooling may be employed to reduce the total thermal gradient. However, in most of the industrial applications AA 6061 is received in pre-treated condition where the option to optimize the solution treatment is not available. Another option is to reheat the material before machining for stress reduction. This way up to 40 % of the residual stresses can be reduced. However, re-heating also drains the material's necessary strength since the material characteristics related to the residual stresses also control the strength mechanism. The objective of this research is therefore to identify a low temperature re-heating that relieves the residual stresses without significant loss of strength.

The reason for reduction in strength after re-heating is the motivation for semi-coherent 13" precipitates to acquire a more stable 13' phase due to increased atomic diffusion. These precipitates now have lesser contribution in strengthening. If the heating further continues the precipitates turn in to a fully distinct 13 phase which has no coherency with the base structure. This distinct phase is unable to arrest the dislocations and only presents physical hindrance to their movement. The material in this condition is said to be over-aged and shows inferior strength. Re-heating at highly elevated temperatures, as experienced during welding, can even dissolve back the secondary precipitates available for strengthening [3]–[6].

Maisonnette et al. studied the coarsening of secondary precipitates with re-heating and identified an average increase in precipitate length and diameter by more than 250% and 64% respectively after re-heating at 400 °C. A strength reduction of about 60% was also observed after re-heating at 450 °C compared to the original T6 state [7]. Lee and Tang have also reported a similar influence of re-heating on AA 6061 alloy. They found re-heating to increase the size of dislocation cells while reducing their number and distribution across the base matrix. This caused the alloy to soften and the flow stress required to continue material deformation at a given strain rate decreased. They identified an average drop in flow stresses by 9.3% when the exposed temperature increased from 100 °C to 200 °C while a further decrease of 16% was recorded at temperatures up to 350 °C [1].

Agarwal et al.found that the secondary precipitates are brittle compared to the base structure and give rise to localized cracks at high loads. These cracks later grow in to voids which play a major part in failure mechanism of AA 6061 alloy [8]. Gharavi et al. identified that the electrochemical potency of these precipitates with respect to the base matrix poses the susceptibility of localized corrosion [9]. De Hass and De Hosson studied the grain boundary

segregation of these precipitates and related it with inter-granular corrosion, a precursor to stress corrosion cracking [10]. All of these studies show the negative consequences of over-precipitation which further affirms the need to keep the re-heating temperature as low as possible for better properties.

Besides the residual stresses induced by thermal gradient the machining induced stresses also take part in material distortions. These stresses are a function of machining parameters, tool and part geometry and the material's inherent properties. Huang et al. found that the effect of machining stresses is greater in thin sections. A sample with a final machined thickness of 0.75 mm deformed approximately 9.8 times that of the 1.75 mm sample [11]. Denkena et al. found that higher cutting speeds lower the final distortions in thin sections [12]. Sridhar and Babu studied the effect of cutting tool dia. on machining distortions. The distortions were found to increase by 41.6% when the cutting tool dia. increased from 6 mm to 16 mm [13].

Since the domain of this study doesn't include optimization of machining parameters the experimental variables are purely related to the re-heating treatment. Different temperatures of re-heating were used keeping the machining parameters and sample geometry as constant. Tests were performed for both the machining distortion and material strength to identify the re-heating temperature that provides the best balance between stress reduction and strength preservation.

2. Experimental Work

Stress relieving for AA 6061 alloy is usually performed through re-heating at 343 °C for 1 hour followed by air cooling [14]. Since this treatment causes extensive degradation of strength 343 °C was set as the maximum experimental temperature. The minimum temperature on the other hand, was set at 240 °C. This is in line of the fact that stress relieving generally starts at 0.45 of the alloy's absolute melting temperature hence much lower temperatures might therefore not be effective for stress relieving [15]. An intermediate temperature of 290 °C was selected to identify the effects in between the maximum and minimum temperatures. The soaking time of 1 hour was not changed since it is fairly standardized. Similarly the quenching medium i.e. still air was also kept constant due to its trivial effect on stress relieving [14] [16]. For each treatment two samples were prepared for both the machining and strength tests. Table I below gives the three selected re-heating treatments for this study.

Table I: Parameters used during the Experiments

Soaking Temperature	Soaking Time	Quenching Medium
343 °C	1 hour	Still Air
290 °C	1 hour	Still Air
240 °C	1 hour	Still Air

2.1 Mechanical Testing

Samples for tensile testing were prepared from a stock piece of raw material as per the ASTM-E8 (Sheet Type) standard. Rough blanks were extracted from the raw material blocks through bend saw machining. It was ensured that all the samples are from the same material orientation to avoid variation of properties. The blanks were than milled to final dimensions of 200x20x10 mm. A dog-bone profile was then prepared with a gauge length of 50 mm. Coolants were used throughout the machining process to minimize the addition of unwanted heat. The samples were tested on a Tinius Olsen H150KU universal testing machine with an Epsilon extensometer attached to measure the elongation before failure. A 0.2% offset method was used to evaluate the yield strength in each tensile test.

The hardness tests were performed on samples extracted from the same blocks as the tensile samples. The testing was performed as per ASTM-E92 (Vicker's) standard on an Ernst bench-type tester.

2.2 Machining Test

The machining test was performed to determine the reduction of machining distortion after re-heating at each of the three selected temperatures. The starting thickness of the samples was kept at 12 mm to avoid any pre-mature distortion. The rectangular shape was selected for the samples due to its ease of preparation from a sheet stock. The length of the samples was kept as much as five times the width in order to mimic a thin long overhang part for prominent effect of distortion.

The samples were re-heated at the three selected temperatures and machining was performed to reduce the thickness up to 2 mm. At this small thickness, the material strength was easily superseded by the residual stresses resulting in distortions. These distortions were then used to relate the effectiveness of each re-heating temperature. As a reference, the pre-machining distortion of each sample was measured using a coordinate measuring machine (CMM). Several readings were made for the sample thickness against a flat base using the machine probe and the thickness was found to vary in the range of 5 to 20 microns. Hence all of the samples were initially flat to reasonable extent.

The machining of the samples was performed using a CNC milling machine with a solid end mill cuter. The machining parameters, as given in Table II below, were selected to avoid large induced stresses. All the samples were clamped from the base using a vice and material was gradually removed from the top side. The machining setup is shown in Figures 1 and 2.

Table II: Process parameters for machining test

Cutter Diameter	10 mm
Cutting Feed	2000 mm / min
Depth of Cut	0.1 mm / pass

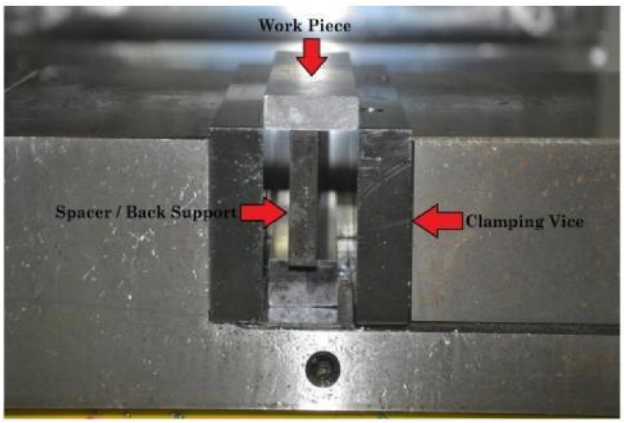

Figure 1: Clamping Setup for Machining

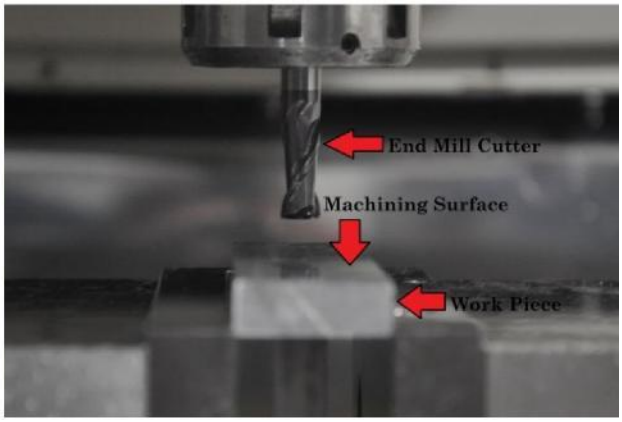

Figure 2: Cutting Tool and the Work Piece

For the after machining distortions the samples were examined on a Starrett Sigma HF600 profile projector shown in Figure 3. The samples were placed on a flat gauge surface and exposed to the light source, as seen in Figure 4. A shadow was then projected on the screen with 5x of magnification. Due to bending, a gap was observed between the sample surface and the relatively flat gauge surface resulting in light to pass through freely. The gap hence appeared as a bright line within the dark image of sample, as shown in Figure 5. By measuring the maximum width of the gap along the image, the magnitude of bending in each sample was determined. This measurement was taken using the built-in mechanism of profile projector.

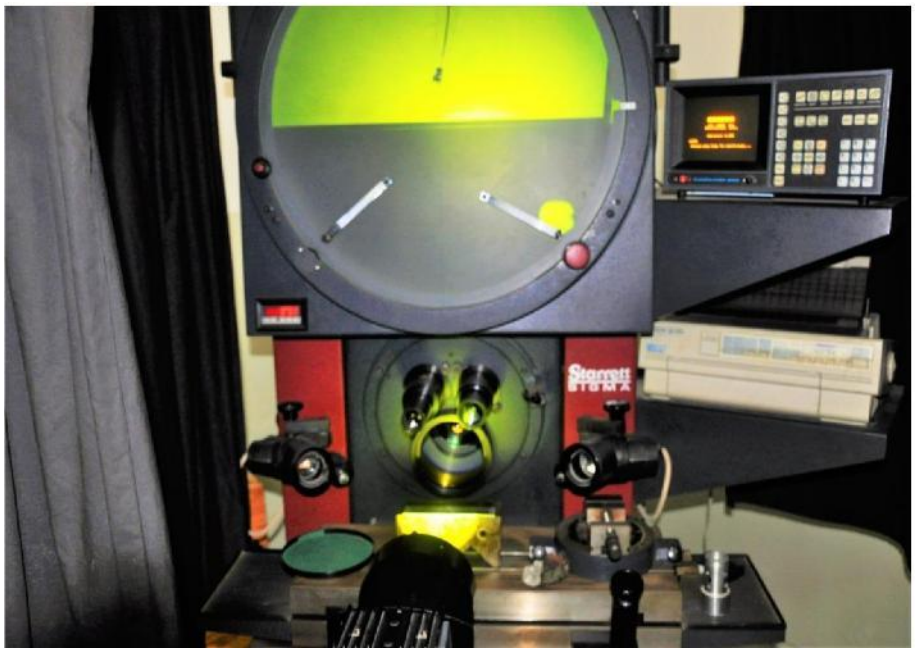

Figure 3: Profile Projector Machine used for Bending Measurements

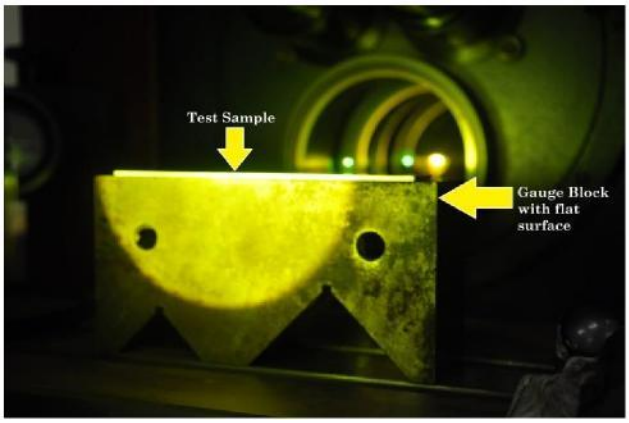

Figure 4: Measuring Setup for Bending

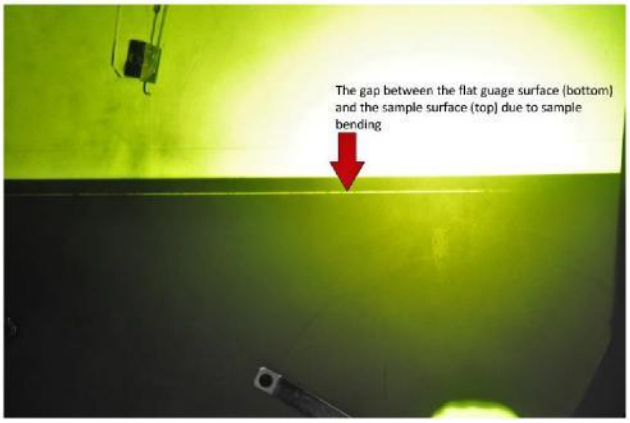

Figure 5: The Gap between the Sample and the Gauge Surface

2.3 Microscopy

Samples with a surface width of 15 mm were used for microscopy in each of the test conditions. The samples were mounted in the bakelite molds and grinded using sand papers starting from 200 to 1200 mesh size and polished with alumina papers starting from 5 to 0.1 microns until a lustrous smooth surface was obtained. The samples were then etched using Keller's reagent to reveal the grain structure. The optical microscopy was performed at OPTIKA B-600 MET equipment with magnifications of 200x, 500x, and 1000x while the electron microscopy was performed at TESCAN Mira3 equipment with higher magnifications of 5000x, 10000x, 25000x and 50000x.

3. Results and Discussion

3.1 Mechanical Testing

The material strength was found to decrease with increasing re-heating temperature, as shown in Figure 6. Compared to the native T6 state, the yield and ultimate tensile strength (UTS) dropped by approximately 62% and 45.8% respectively after re-heating at 343 °C. This reflects on the effect of precipitate coarsening and dislocation redistribution explained earlier [1], [7]. Re-heating at 240°C resulted in a mild drop of 1.8% and 5.6% in yield strength and UTS respectively. This indicates small-scale structural changes at this temperature. A similar pattern was observed in the hardness tests with an approximate drop of 50% after re-heating at 343 °C compared to the T6 state, as shown in Figure 7. In contrast the ductility was found to be mildly changed up till 290 °C after which it shoots by up to 51.8% of the original T6 condition at the reheating temperature of 343 °C. Figure 8 shows the change of ductility with respect to the reheating temperature.

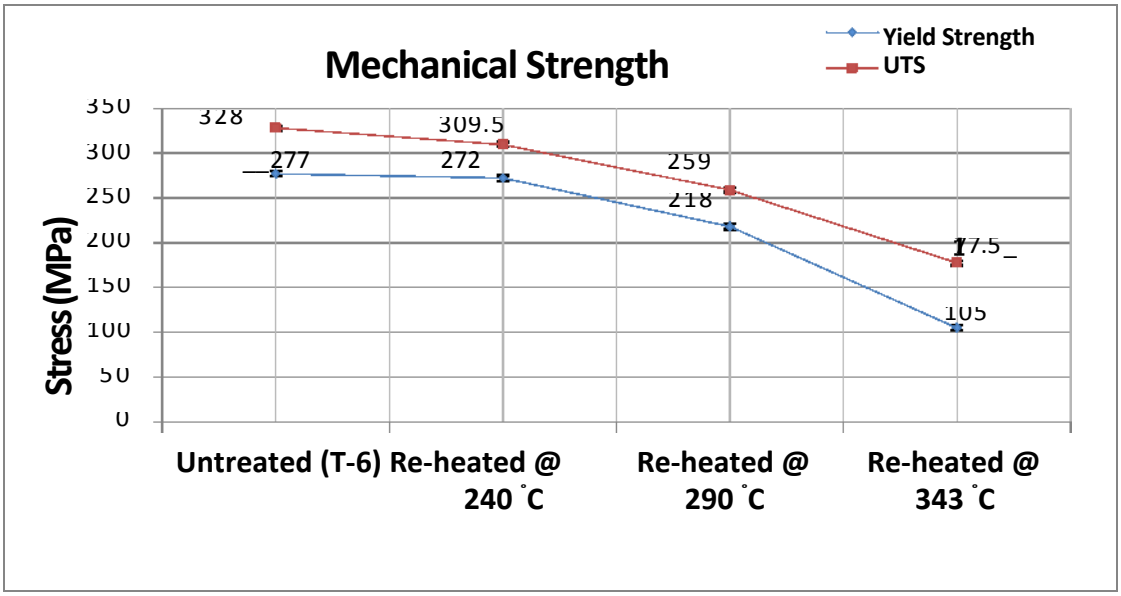

Figure 6: Tensile Test Results for Original T6 and Re-heated Conditions at different Temperatures

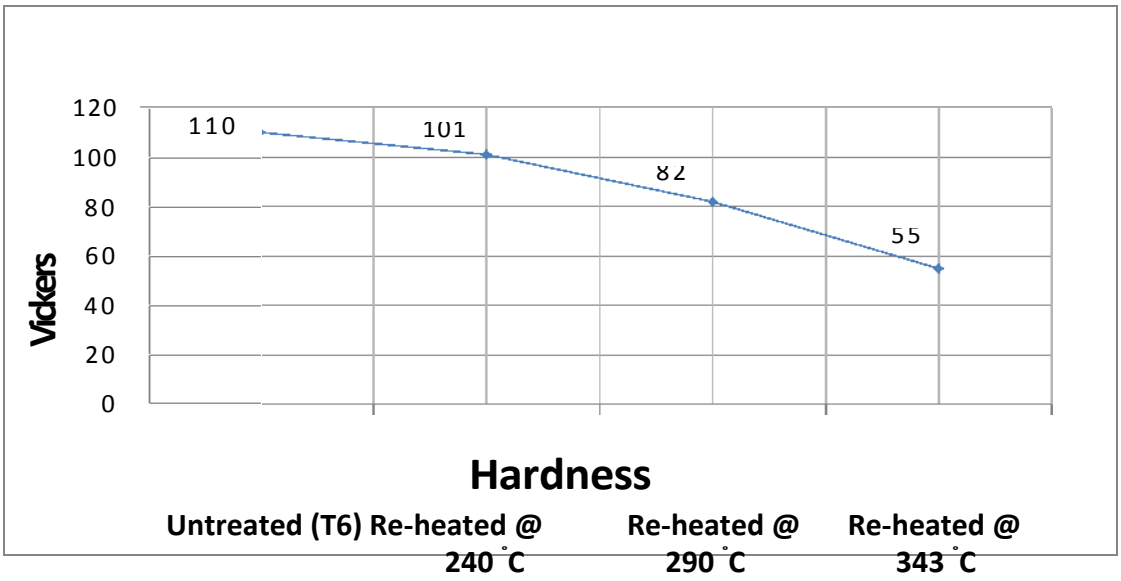

Figure 7: Hardness for original T6 and re-heated conditions at different temperatures

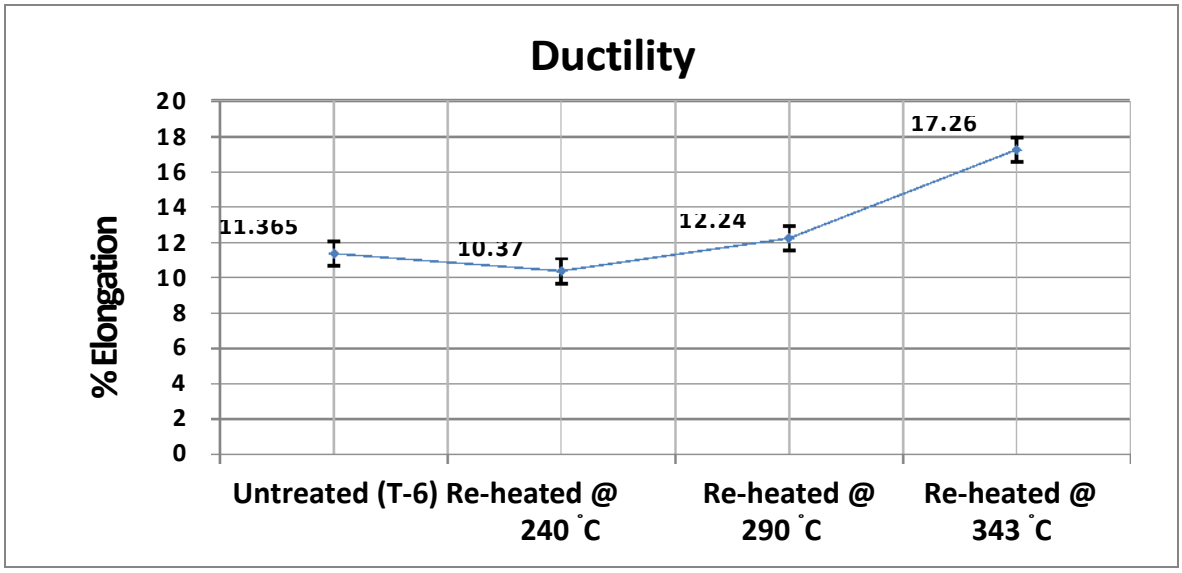

Figure 8: % Elongation for Original T6 and Re-heated Conditions at different Temperatures

3.2 Machining Test

The results of the machining test together with the mechanical testing are summarized in Table III. The table values are the average of two samples for each testing condition. The highest distortions were achieved at re-heating temperature of 240˚C which is almost similar to the untreated condition. The samples treated at 290 ˚C exhibited the lowest distortion while re-heating at 343˚C yielded intermediate results. Figure 9 shows after machining distortions for each of the three re-heating conditions and the original T6 state.

Table III: Summary of mechanical testing and machining distortion

Material Condition	Mechanical Strength (MPa)		Hardness (Vicker's)	Machining % Elongation	Distortions (mm)
	Yield Stress	UTS			
Untreated (T6)	277	328	110	11.365	0.428
Re-heated @ 240 ˚C	272	309.5	101	10.37	0.415
Re-heated @ 290 ˚C	218	259	82	12.24	0.161
Re-heated @ 343 ˚C	104.95	177.55	55	17.26	0.301

The results indicate that while higher temperature caused greater material softening, it was not equally effective in preventing the machining distortion. As mentioned earlier, the distortions are a combined effect of residual stresses both from the previous processing and the machining itself. Lower part thickness (below 2 mm) is particularly prone to distortion due to decreased material resistance [11] [12]. Although re-heating at 343 °C relaxed the thermally induced stresses, the accompanied material softening favored the machining stresses due to which better results could not be achieved. It is observed that re-heating at 290 °C balanced the two stresses well thereby improving the machining distortions. The distortions were reduced by up to 60% at 290 °C with a corresponding decrease of 21% in strength. This is a workable solution for machining applications where slight loss of strength is tolerable. Re-heating at 240 °C was found to bring insignificant structural changes for considerable improvement in distortion.

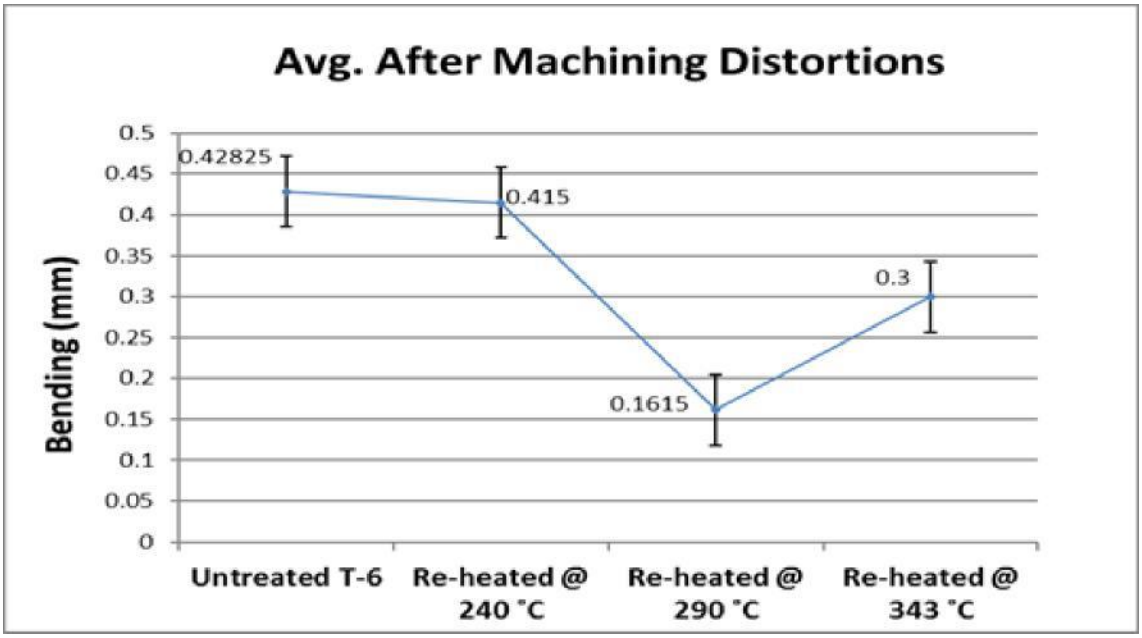

Figure 9: After machining Distortions for Original T6 and Re-heated Conditions at different Temperatures

3.3 Microscopy

The results of both optical and electron microscopy show the sensitivity of secondary precipitates with respect to the re-heating temperature. The main factors which influence reheating are coarsening of strengthening precipitates due to increased atomic diffusion, annihilation and redistribution of the dislocation cells, and the dissolution of existing precipitates at higher temperature [1] [6] [7].

Figure 10 shows the optical micrographs at 1000x magnification for samples in original T6 and re-heated condition at the three selected soaking temperatures. The arrows in Figure 10 point

towards over-aging in the form of increased black phase density as the re-heating temperature is increased. This black color is characteristic of Mg_2Si precipitates which take part in strengthening [9] [17].

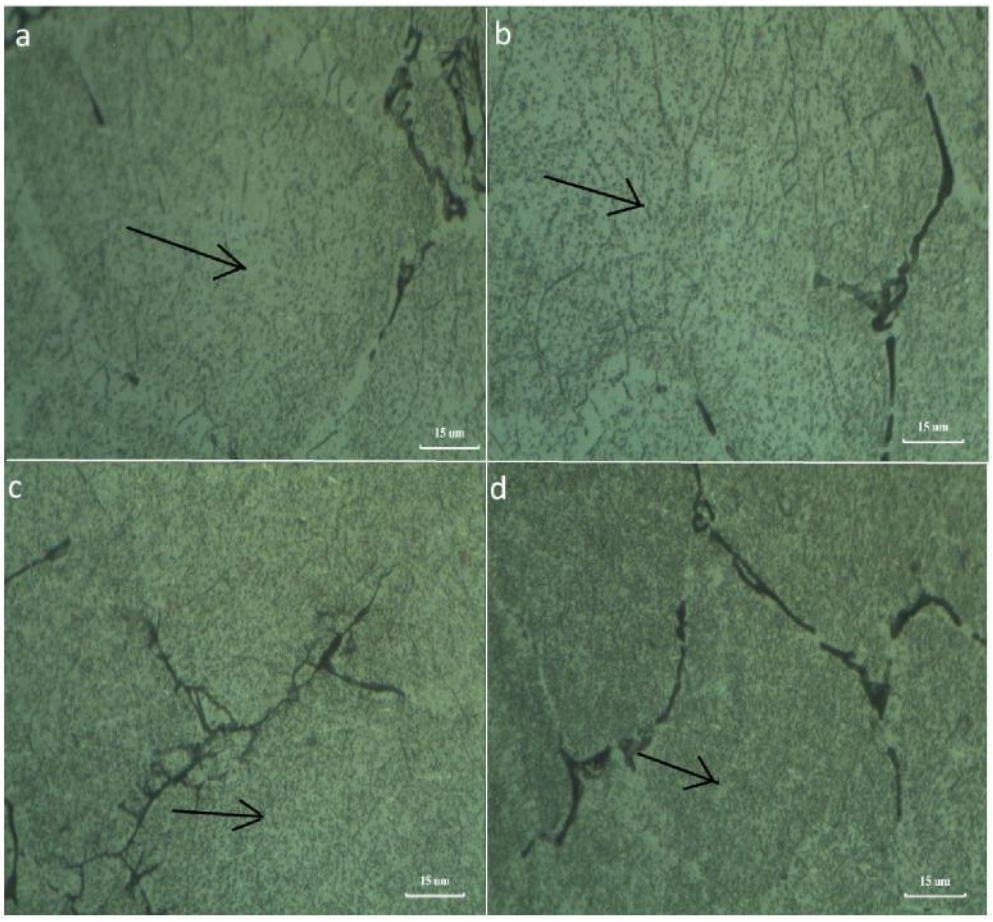

Figure 10: (a) Original T6 State (b) Re-heated at 240 ˚C(c) Re-heated at 290 ˚C (d) Re-heated at 343 ˚C

The micrographs also reveal the dissolution of precipitate clusters from the grain boundaries after re-heating at 343 ˚C, as shown in Figure 11. This effect is not visible at 240 ˚C and 290 ˚C. These clusters are a major cause of inter-granular corrosion leading to stress corrosion cracking [10]. The presence of these clusters at grain boundaries however, provides added reinforcement and their dissolution further eases dislocation movement. This is one of the reasons for a 50% drop in material strength after re-heating at 343 ˚C. Figure 11a shows the grain boundary precipitates in T6 condition while Figure 11b shows their dissolution after reheating at 343 ˚C.

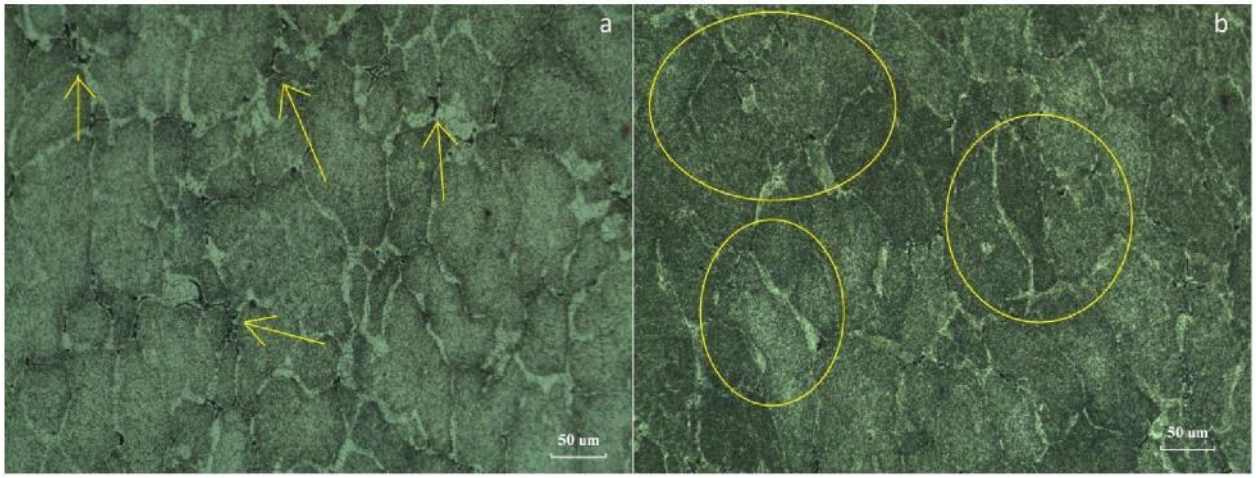

Figure 11: Depletion of Grain Boundary Precipitates after Re-heating above 300 ˚C

Figure 12 to 15 show the electron micrographs at 25000x magnification for samples in original T6 and re-heated conditions. The precipitates are now better resolved and an increase in their density and size can be seen with an increase in re-heating temperature. As the precipitates grow larger, their coherency with the base structure is lost resulting in a decrease in strength. The micrograph of re-heated condition at 343 ˚C again shows precipitate depleted grain boundaries as seen in Figure 15. The micrographs of original T6 and re-heated condition at 240 ˚C have similar structural characteristics, as seen in Figure 12 and 13, which explains the minimal difference of properties between the two conditions.

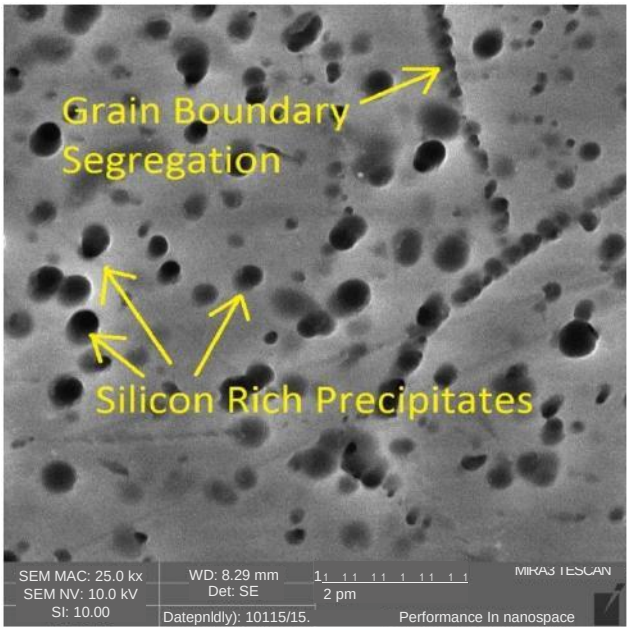

Figure 12: Original T6 State

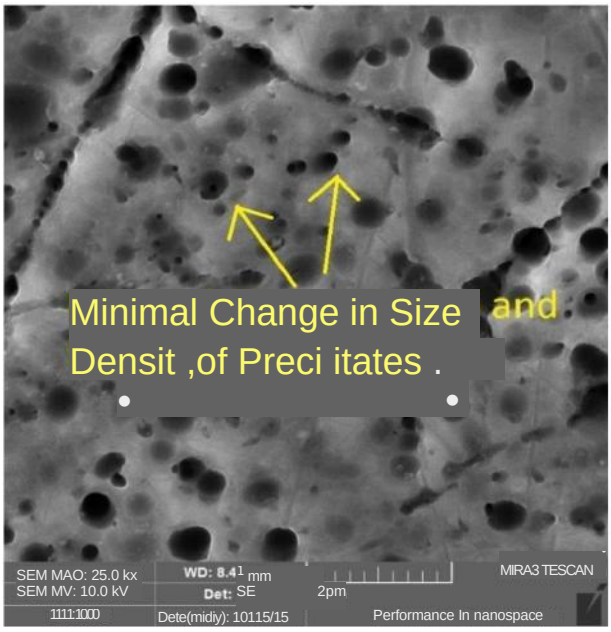

Figure 13: Re-heated at 240 ˚C

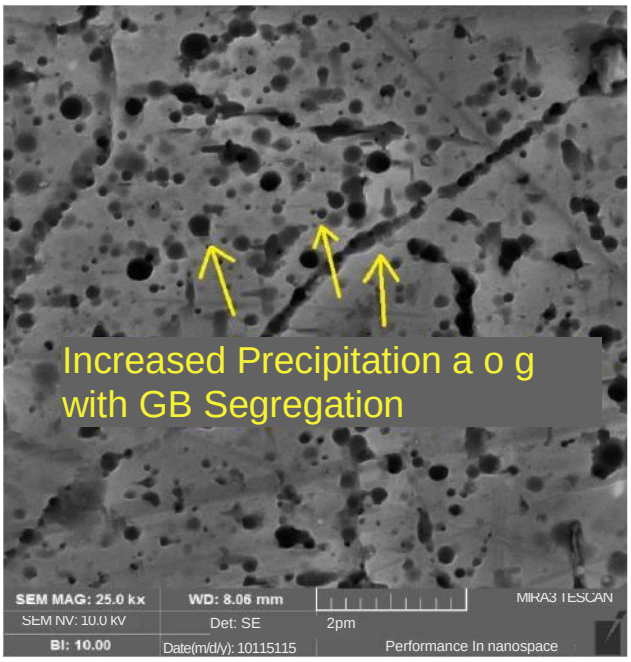

Figure 14: Re-heated at 290 ˚C

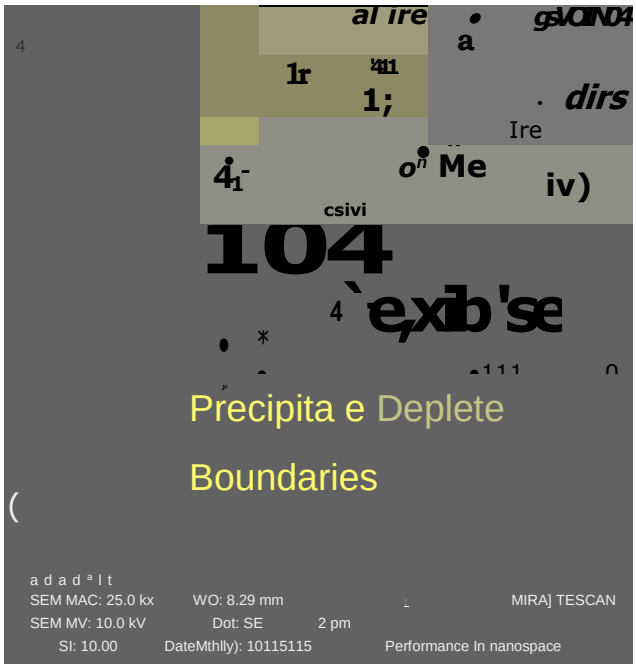

Figure 15: Re-heated at 343 ˚C

4. Conclusions

Re-heating reduces residual stresses for lesser distortions during the machining however it also lowers the material strength by directly affecting the secondary precipitates. This effect is proportional to the re-heating temperature hence lower temperatures are always preferable for re-heating.

Re-heating temperature above 300 °C can reduce the strength of AA 6061 alloy by more than 50% with a simultaneous increase in ductility while re-heating below 240 °C is found to be ineffective to induce sufficient structural changes for stress reduction. Re-heating temperature of 290 °C was found to be the most effective in reducing machining distortions. The distortions were reduced up to more than 60% with a corresponding decrease in strength of 21%.

Both optical and electron micrographs reveal an increase in size and density of silicon rich strengthening precipitates with an increase in re-heating temperature. The difference in the mechanical properties and structural characteristics of original and re-heated condition at 240 °C was found to be insignificant.

Acknowledgement

Financial support for this work by the National University of Sciences and Technology of Pakistan is gratefully acknowledged. The authors are utterly thankful to Mr. Naveed Hassan Siddiqui (*Delft University of Technology, Delft, Netherlands*) for his continual support and supervision throughout the course of study.

References

[1] W.-S. Lee and Z.-C. Tang, “Relationship between mechanical properties and microstructural response of 6061-T6 aluminum alloy impacted at elevated temperatures,” *Mater. Des.*, vol. 58, pp. 116–124, Jun. 2014.

[2] G. P. Dolan and J. S. Robinson, “Residual stress reduction in 7175-T73, 6061-T6 and 2017A-T4 aluminium alloys using quench factor analysis,” *J. Mater. Process. Technol.*, vol. 153–154, no. 1–3, pp. 346–351, 2004.

[3] P. DeGarmo, J. T. Black, and R. Kohser, *Materials and Processes in Manufacturing*, Ninth. Michigan: Wiley, 2003.

[4] H. Chandler, *Heat Treater’s Guide: Practices and Procedures for Nonferrous Alloys*. Ohio: ASM International, 1996.

[5] S. P. Ringer and K. Hono, “Microstructural Evolution and Age Hardening in Aluminium Alloys,” *Mater. Charact.*, vol. 44, no. 1–2, pp. 101–131, Jan. 2000.

[6] D. Peng, J. Shen, Q. Tang, C. Wu, and Y. Zhou, “Effects of aging treatment and heat input

on the microstructures and mechanical properties of TIG-welded 6061-T6 alloy joints," *Int. J. Miner. Metall. Mater.*, vol. 20, no. 3, pp. 259–265, Mar. 2013.

[7] D. Maisonnette, M. Suery, D. Nelias, P. Chaudet, and T. Epicier, "Effects of heat treatments on the microstructure and mechanical properties of a 6061 aluminium alloy," *Mater. Sci. Eng. A*, vol. 528, no. 6, pp. 2718–2724, Mar. 2011.

[8] H. Agarwal, A. . Gokhale, S. Graham, and M. . Horstemeyer, "Void growth in 6061-aluminum alloy under triaxial stress state," *Mater. Sci. Eng. A*, vol. 341, no. 1–2, pp. 35– 42, Jan. 2003.

[9] F. Gharavi, K. A. Matori, R. Yunus, N. K. Othman, and F. Fadaeifard, "Corrosion behavior of Al6061 alloy weldment produced by friction stir welding process," *J. Mater. Res. Technol.*, vol. 4, no. 3, pp. 314–322, Jul. 2015.

[10] M. De Hass and J. T. M. De Hosson, "Grain boundary segregation and precipitation in aluminium alloys," *Scr. Mater.*, vol. 44, no. 2, pp. 281–286, 2001.

[11] X. Huang, J. Sun, and J. Li, "Effect of Initial Residual Stress and Machining-Induced Residual Stress on the Deformation of Aluminium Alloy Plate," *Strojniški Vestn. – J. Mech. Eng.*, vol. 61, no. 2, pp. 131–137, 2015.

[12] B. Denkena, L. De León-García, and J. Köhler, "Influence of High Performance Cutting Operations on the Residual Stresses of Aluminum Structural Work-pieces," in *25th International Congress of the Aeronautical Sciences*, 2006.

[13] Sridhar G. and Ramesh Babu P., "Effect of a milling cutter diameter on distortion due to the machining of thin wall thin floor components", *APEM Journal,* vol. 10, no. 3, pp. 140152, (2015).

[14] Military Standardization Handbook MI1-HDBK-694A(MR), "Aluminum and Aluminum Alloys", *US Army Material Research Agency*, Department of Defense, Washington 25 D.C., (1966), available from: http://www.everyspec.com.

[15] Mandy S. Younger and Kenneth H. Eckelmeyer, "Overcoming Residual Stresses and Machining Distortion in the Production of Aluminum Alloy Satellite Boxes", *Sandia National Laboratories Report (SAND2007-6811)*, Sandia Corporation, US Department of Energy, (2007), available from: http://prod.sandia.gov/techlib/access-control.cgi/2007/076811.pdf.

[16] Aerospace Material Specification (AMS 2700H), "Heat Treatment of Wrought Aluminum Alloy Parts", *SAE Aerospace* ,(2006), available from: http://www.jnhaide.com/4456C374-969E-41C7-AEBF-8E7A07FCE5EF/FinalDownload/DownloadId-75416E3C472BAF97EF1125324EB67191/4456C374-969E-41C7-AEBF-8E7A07FCE5EF/pdf/AMS2770H.pdf.

[17] J. Zhang, Z. Fan, Q. Wang and L. Zhou, "Equilibrium Pseudo-binary Al-Mg2Si Phase Diagram", *Mater. Sci. Technol.*, vol. 17, No. 5, p. 494-496, (2001), available from: https://www.brunel.ac.uk/data/assets/pdffile/0004/295366/Equilibrium-pseudo-binary.pdf.

Figure 1

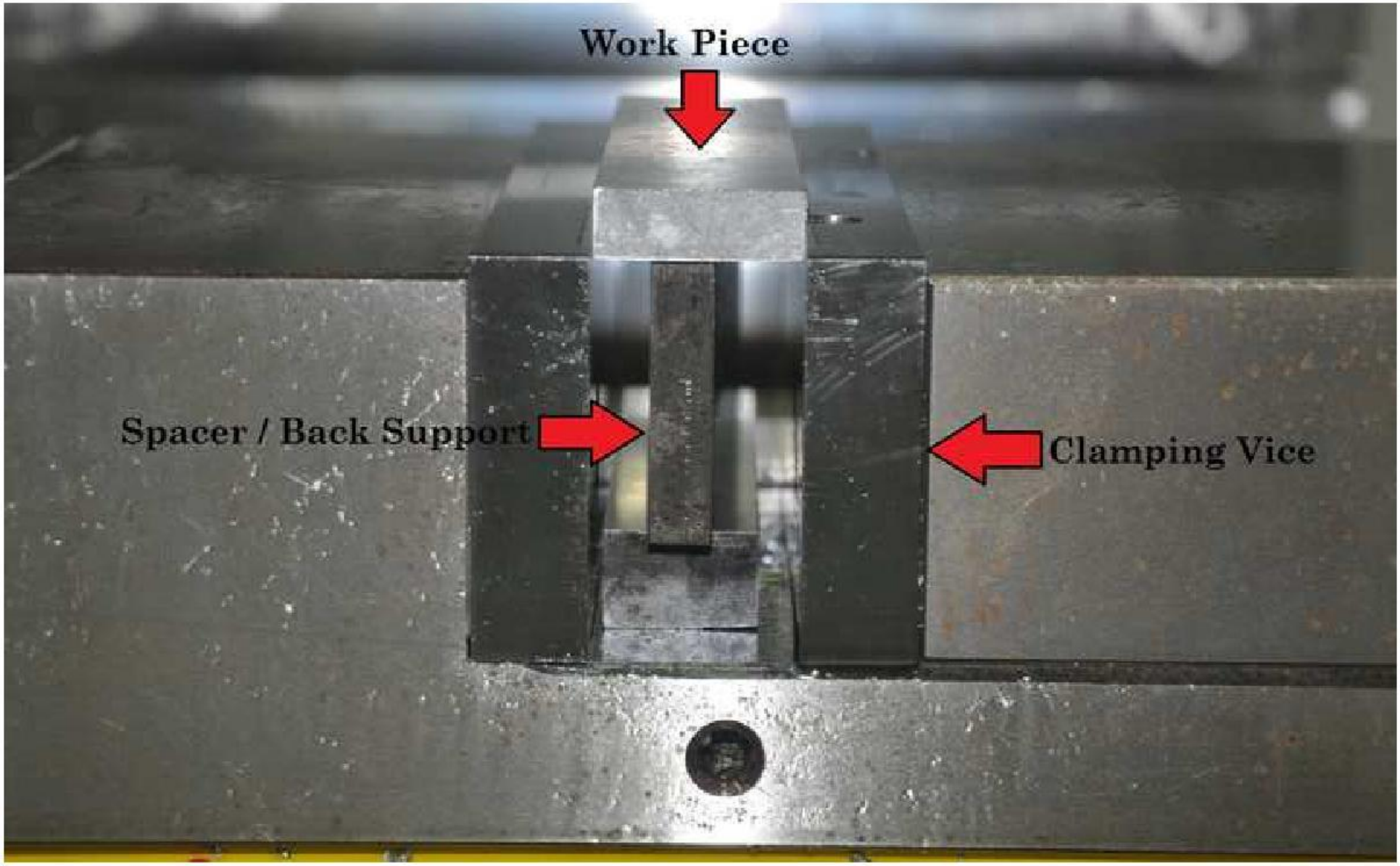

Figure 2

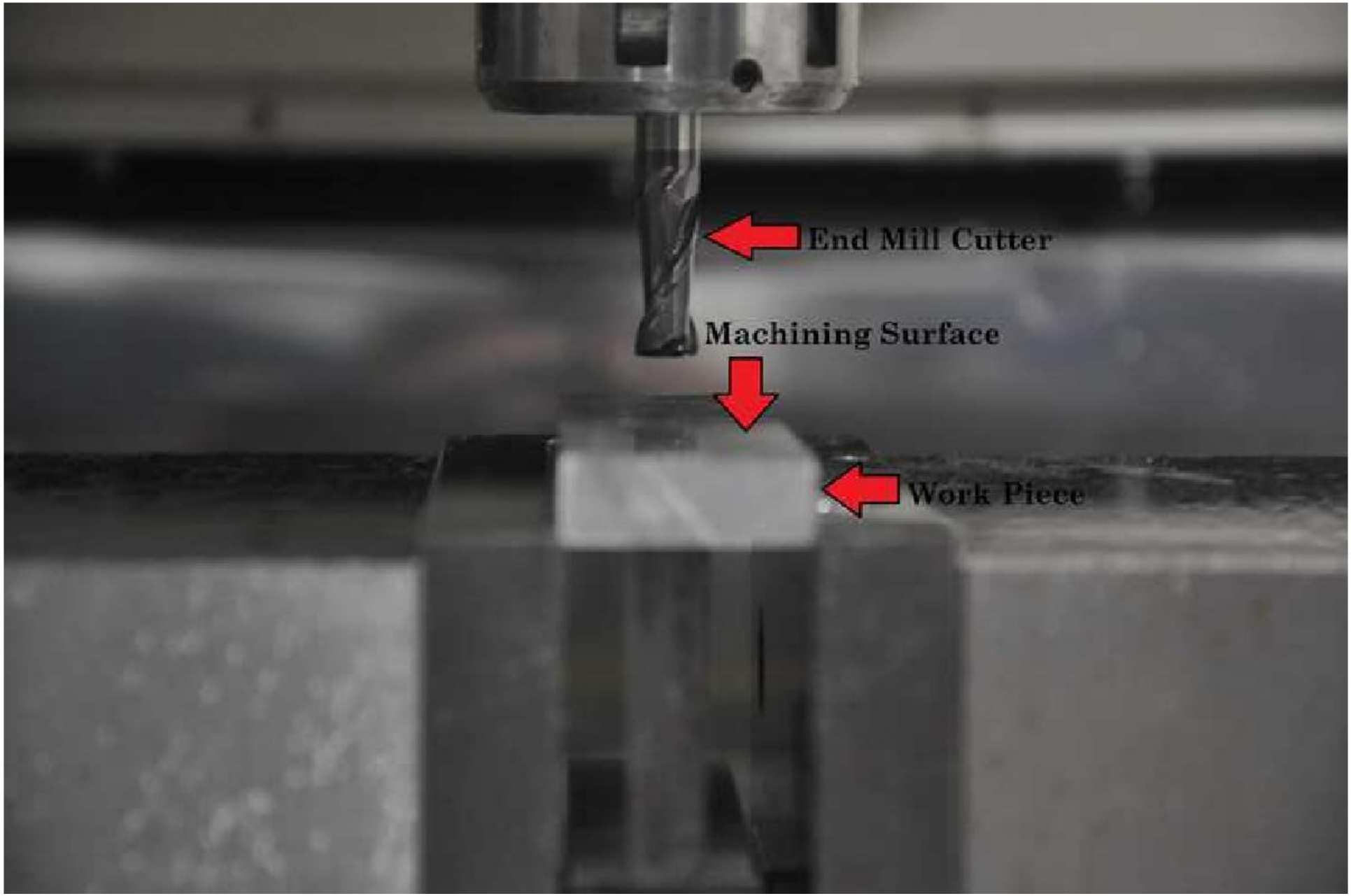

Figure 3

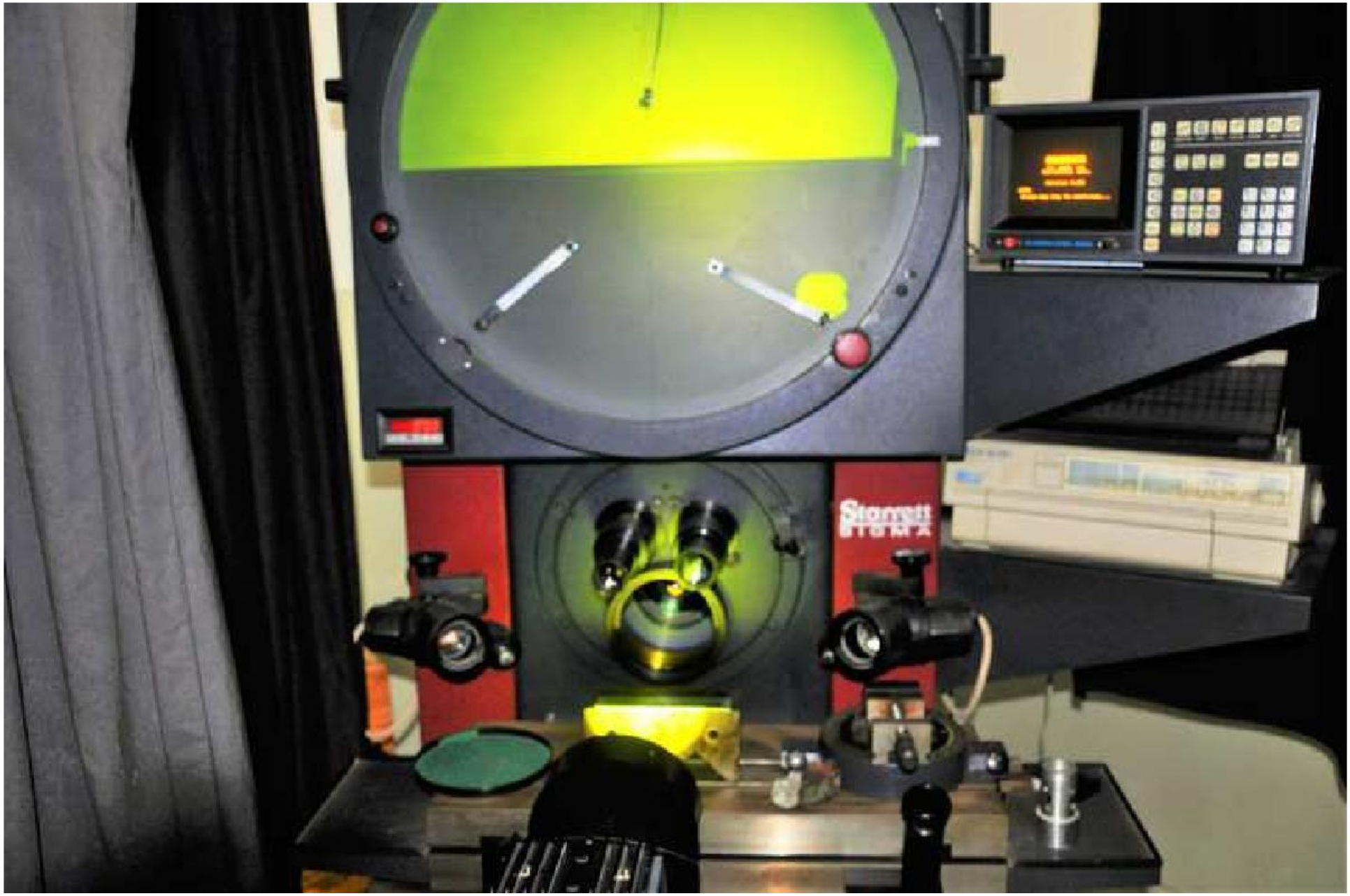

Figure 4

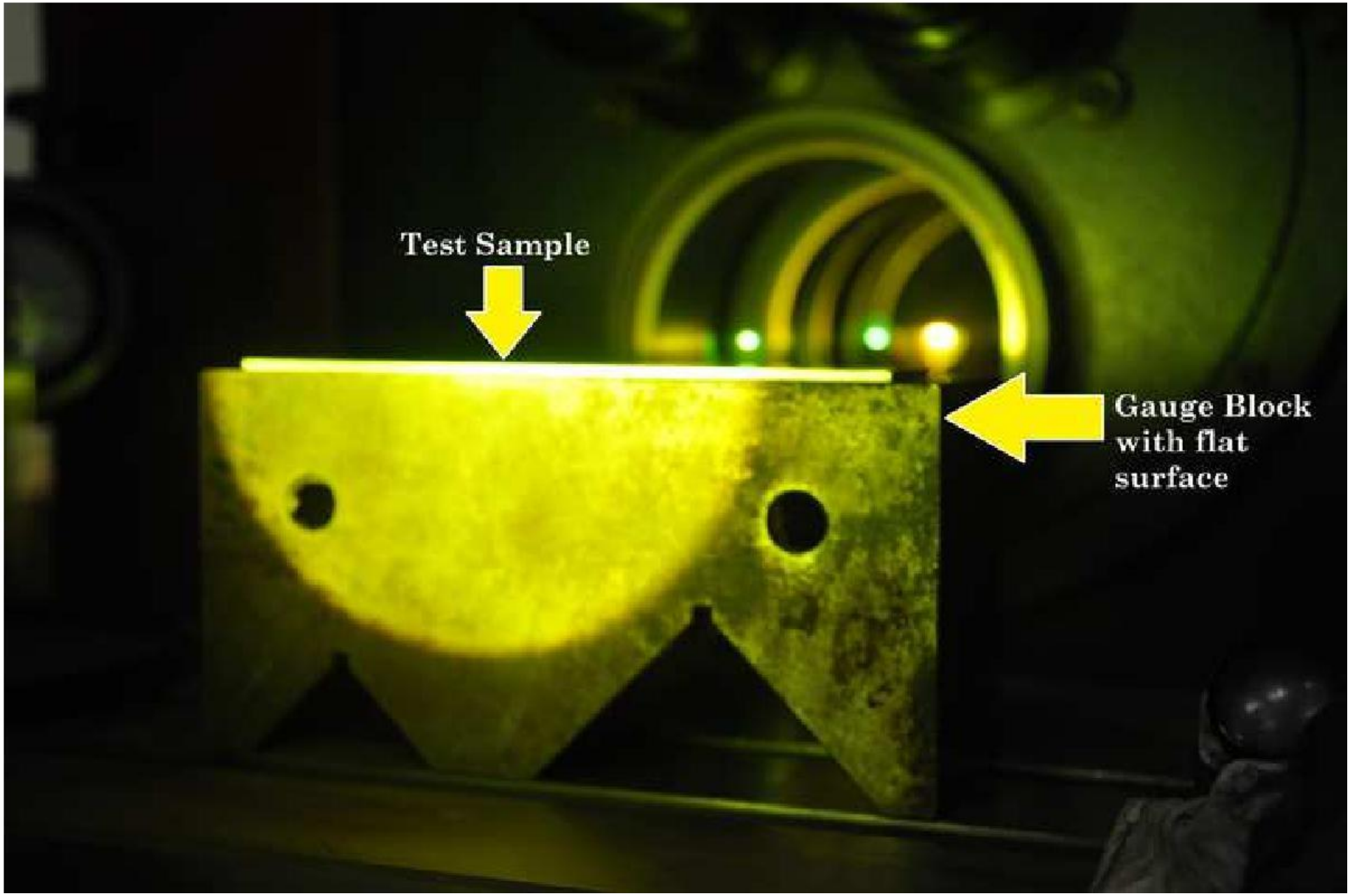

Figure 5

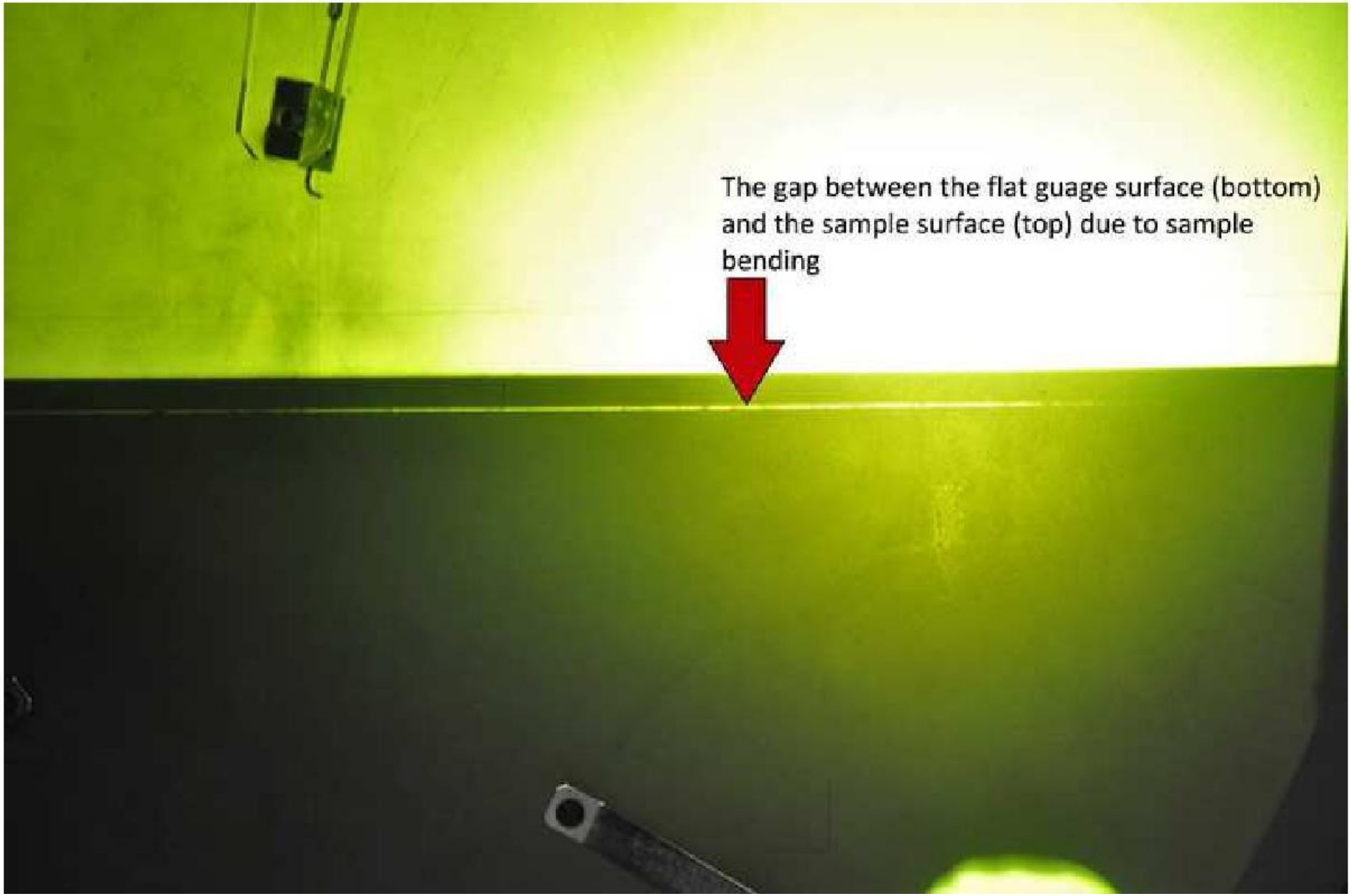
The gap between the flat guage surface (bottom) and the sample surface (top) due to sample bending

Figure 6

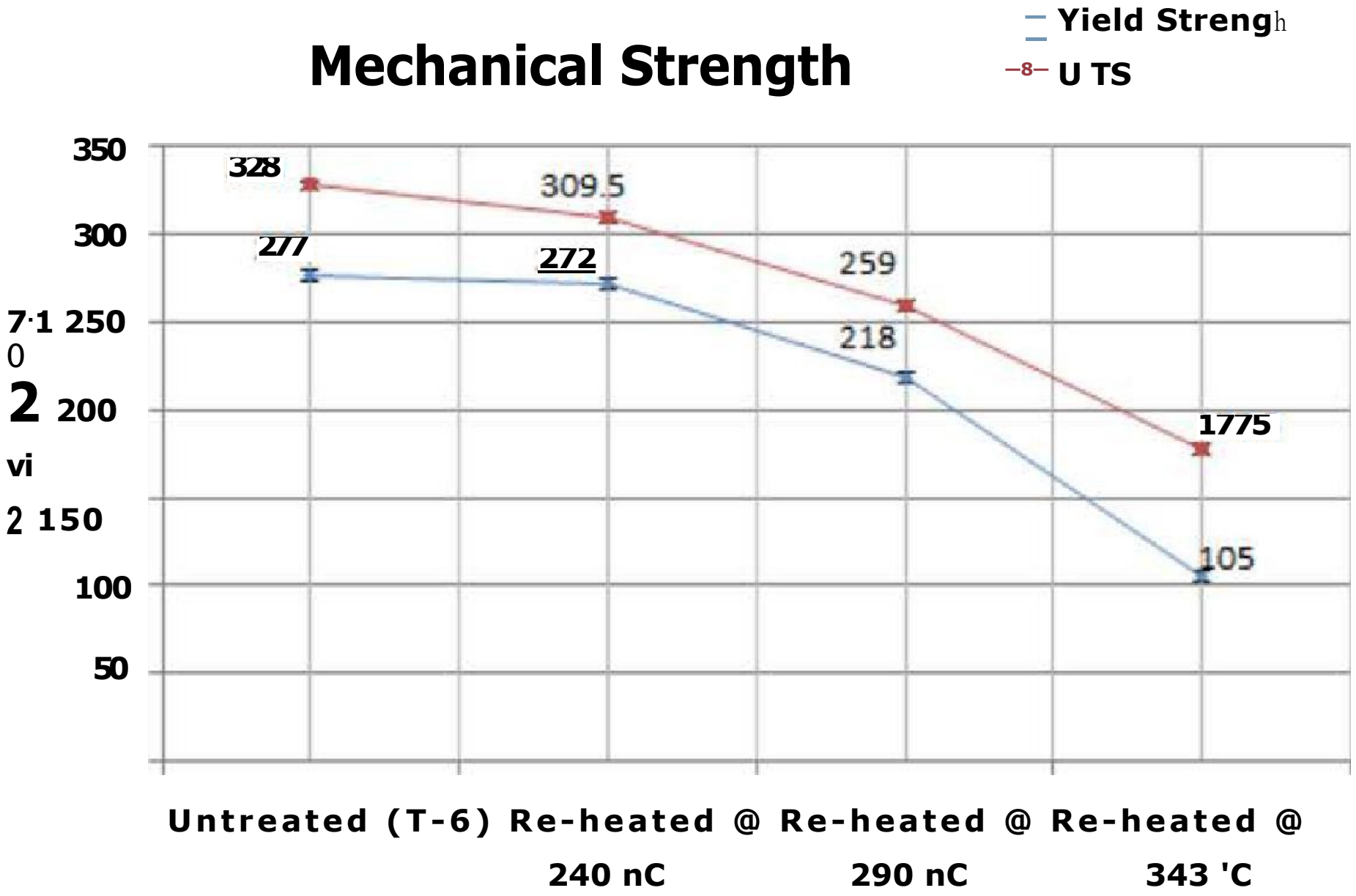
Mechanical Strength
Yield Strengh
U TS
350
300
250
200
150
100
50
328
309.5
277
272
259
218
1775
105
Untreated (T-6)
Re-heated @ 240 nC
Re-heated @ 290 nC
Re-heated @ 343 'C

Figure 7

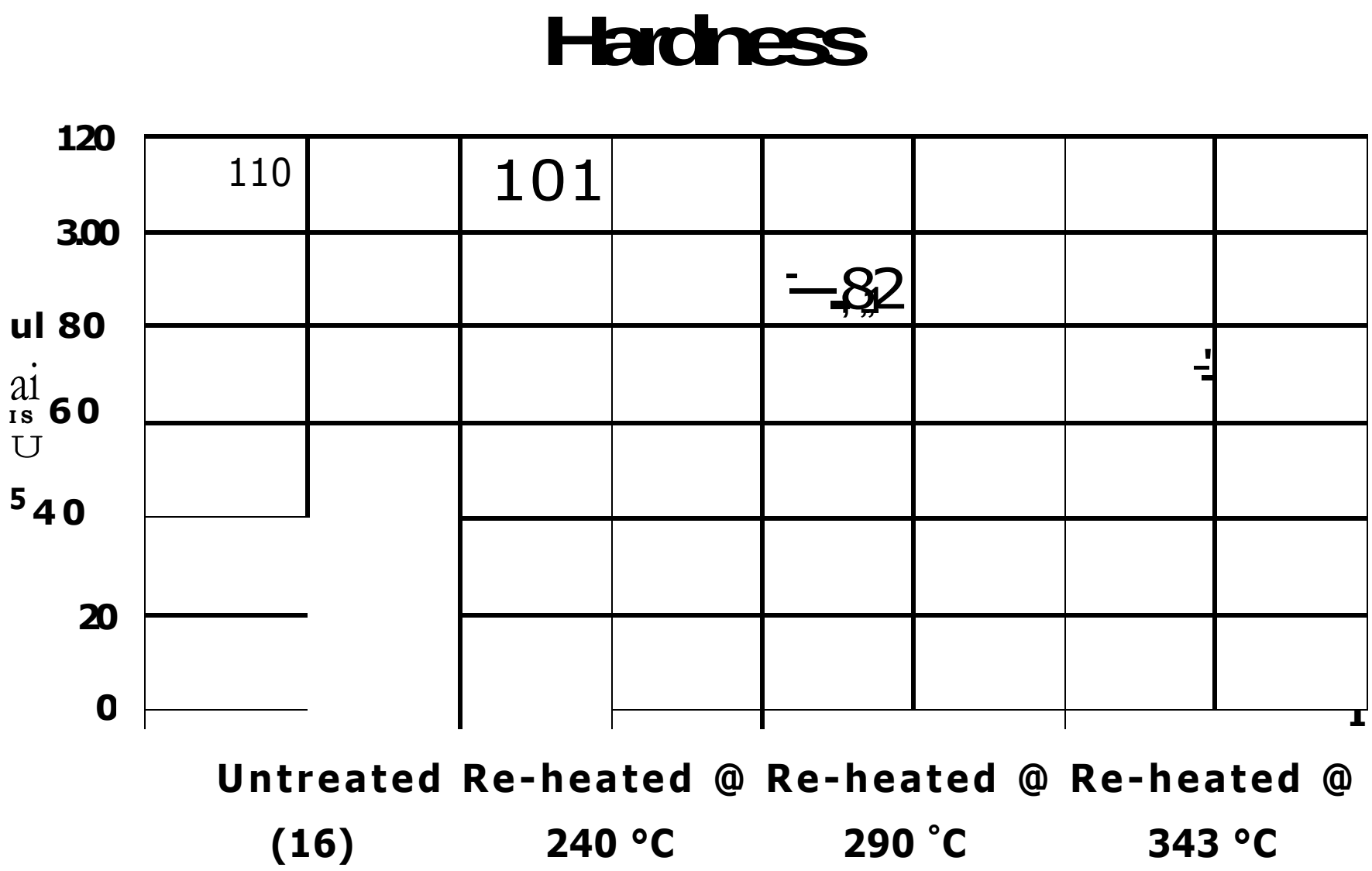
Hardness
120
100
80
60
40
20
0
110
101
82
Untreated (16)
Re-heated @ 240 °C
Re-heated @ 290 °C
Re-heated @ 343 °C

Figure 8

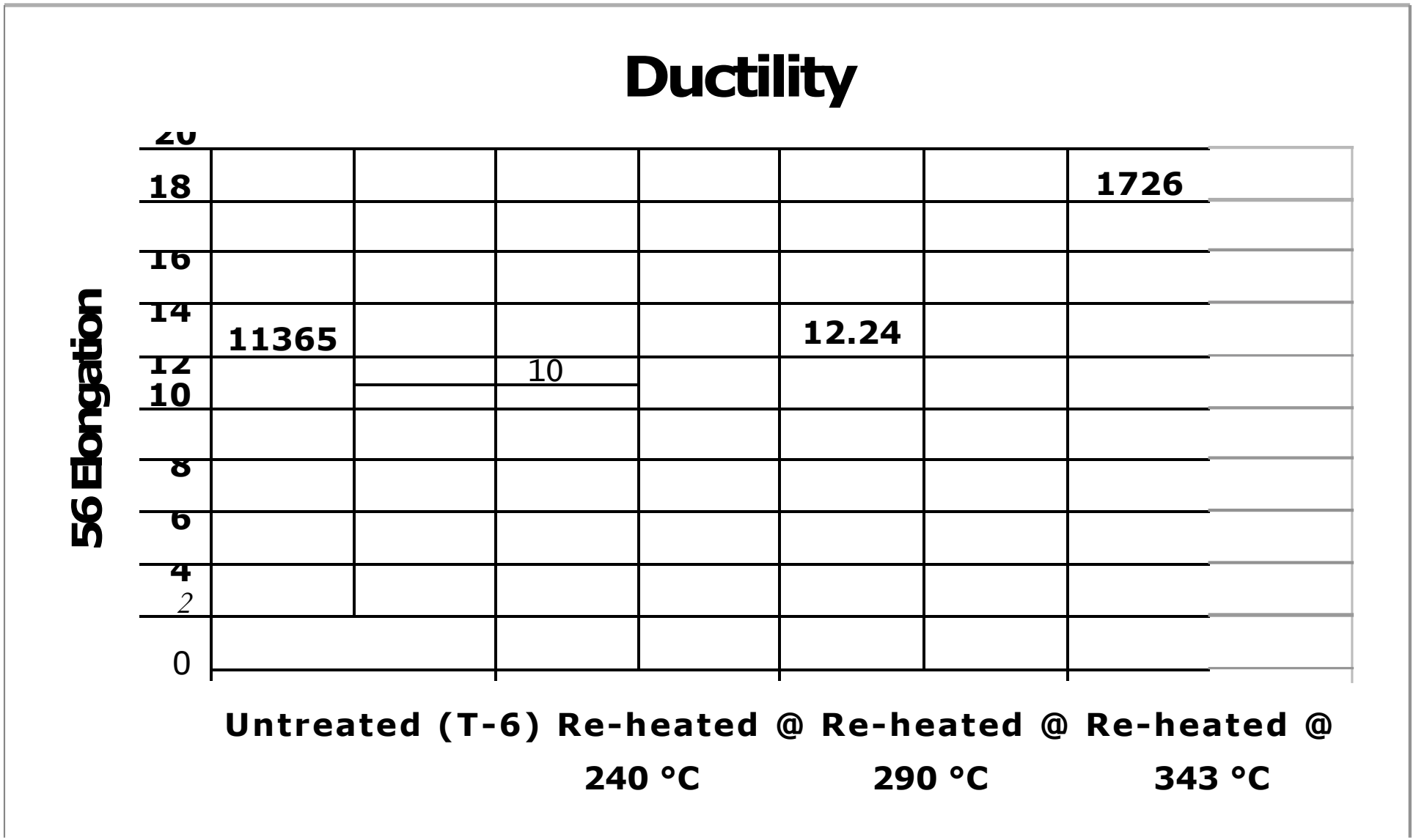
Ductility
56 Elongation
20
18
16
14
12
10
8
6
4
2
0
11365
10
12.24
1726
Untreated (T-6)
Re-heated @ 240 °C
Re-heated @ 290 °C
Re-heated @ 343 °C

Figure 9

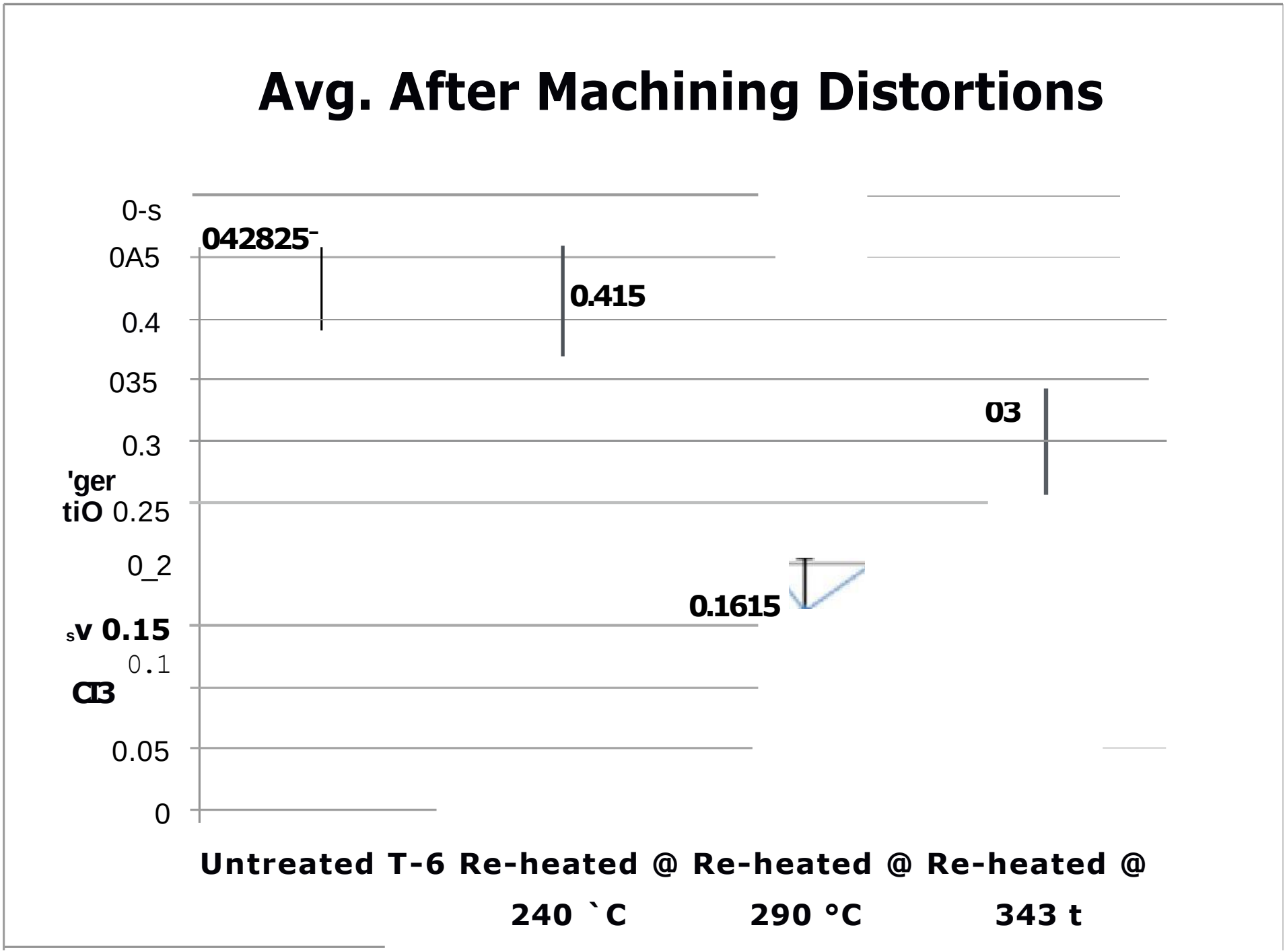
Avg. After Machining Distortions
0-s
042825-
0A5
0.415
0.4
035
03
0.3
'ger
tiO 0.25
0_2
0.1615
sv 0.15
0.1
CI3
0.05
0
Untreated T-6
Re-heated @ 240 `C
Re-heated @ 290 °C
Re-heated @ 343 t

Figure 10

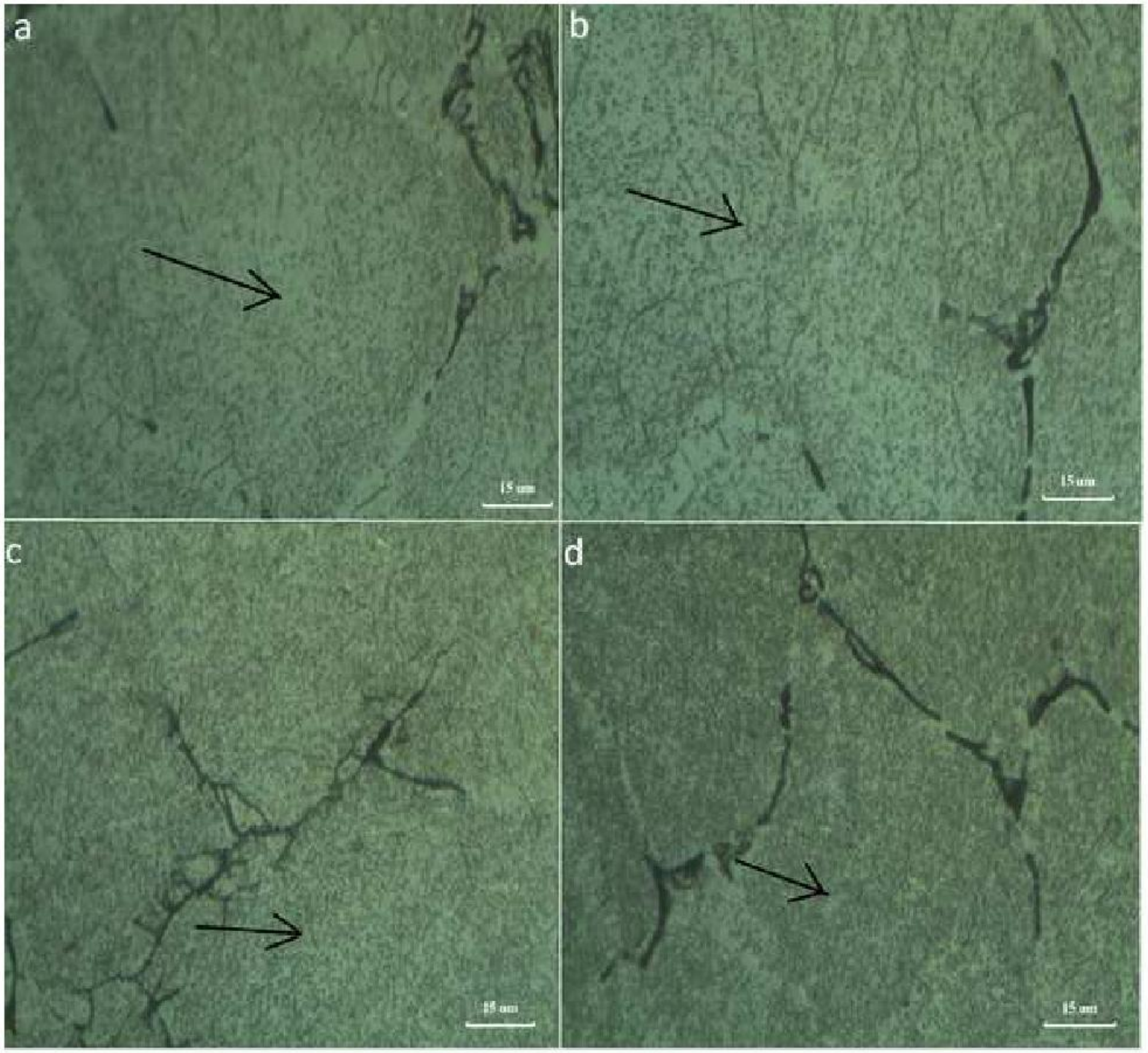

Figure 11

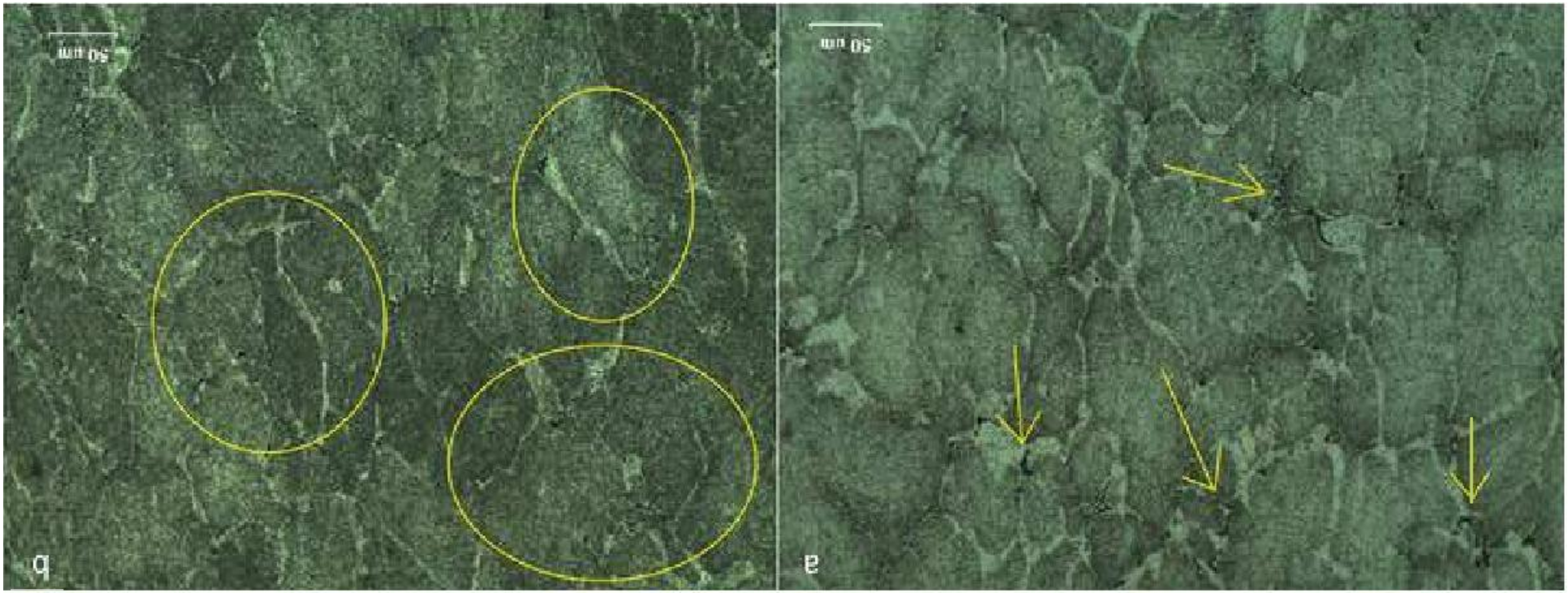

Figure 12

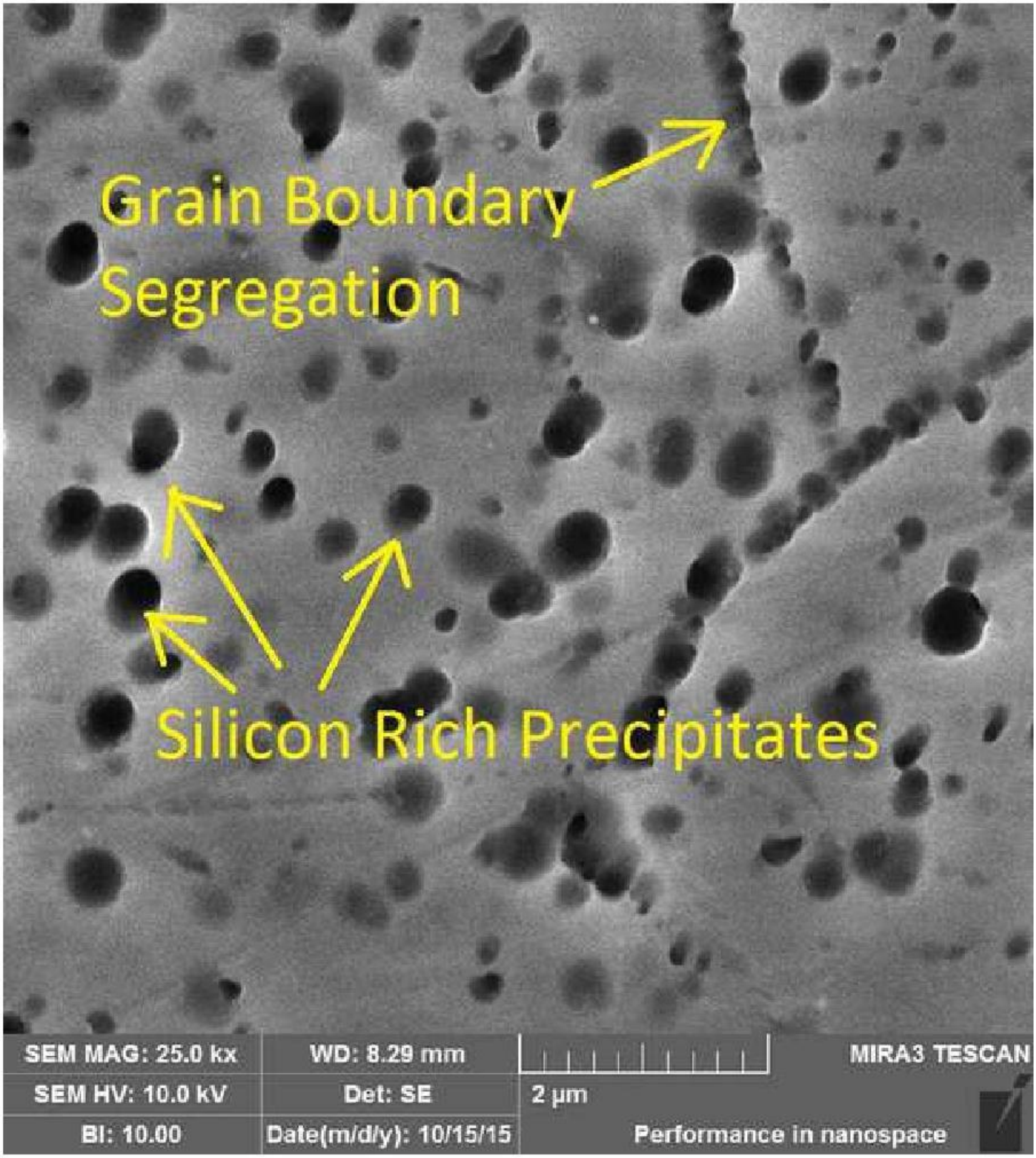
Grain Boundary Segregation
Silicon Rich Precipitates
SEM MAG: 25.0 kx
WD: 8.29 mm
MIRA3 TESCAN
SEM HV: 10.0 kV
Det: SE
2 µm
BI: 10.00
Date(m/d/y): 10/15/15
Performance in nanospace

Figure 13

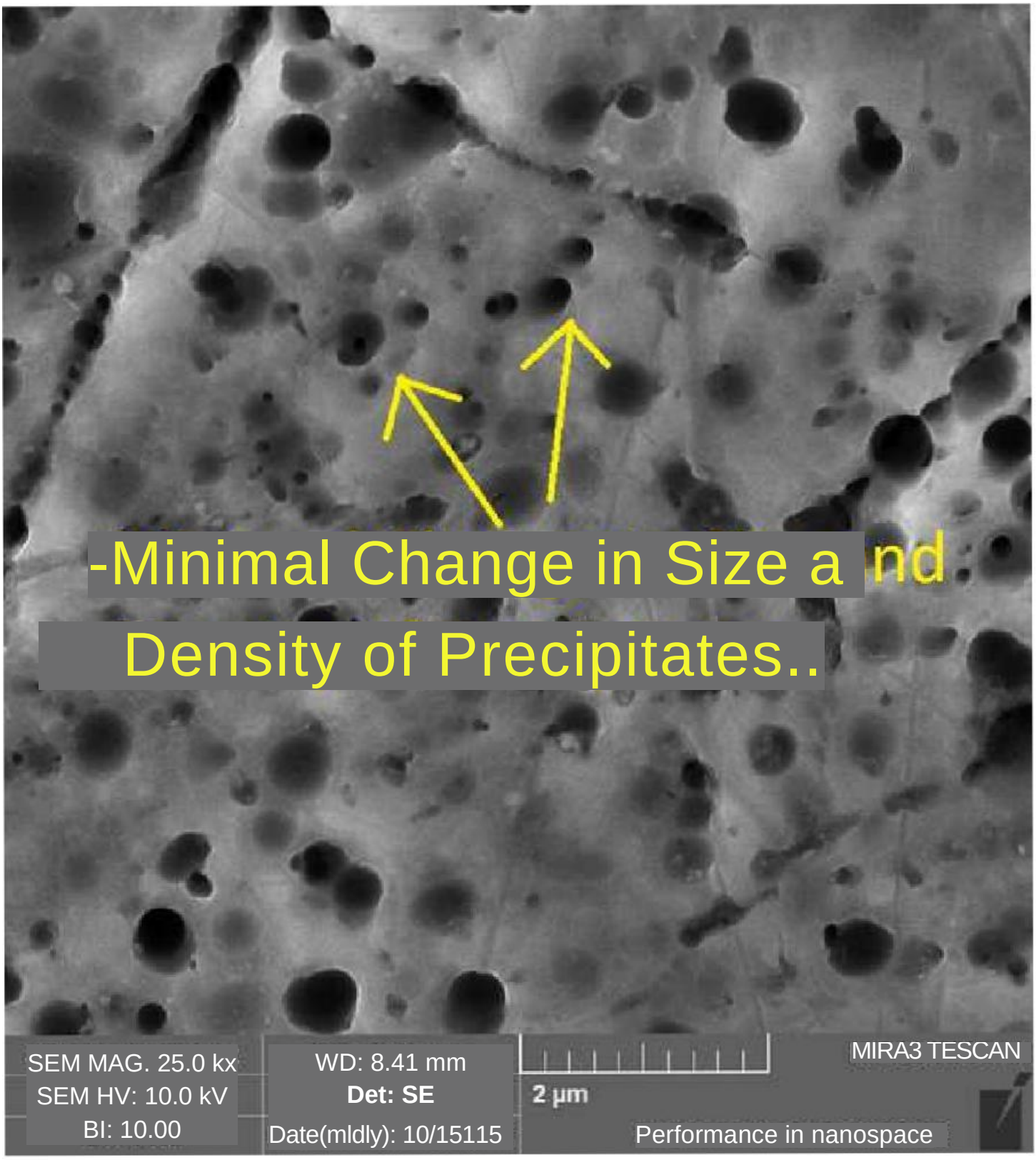
-Minimal Change in Size a nd
Density of Precipitates..
SEM MAG. 25.0 kx
SEM HV: 10.0 kV
BI: 10.00
WD: 8.41 mm
Det: SE
Date(mldly): 10/15115
2 µm
MIRA3 TESCAN
Performance in nanospace

Figure 14

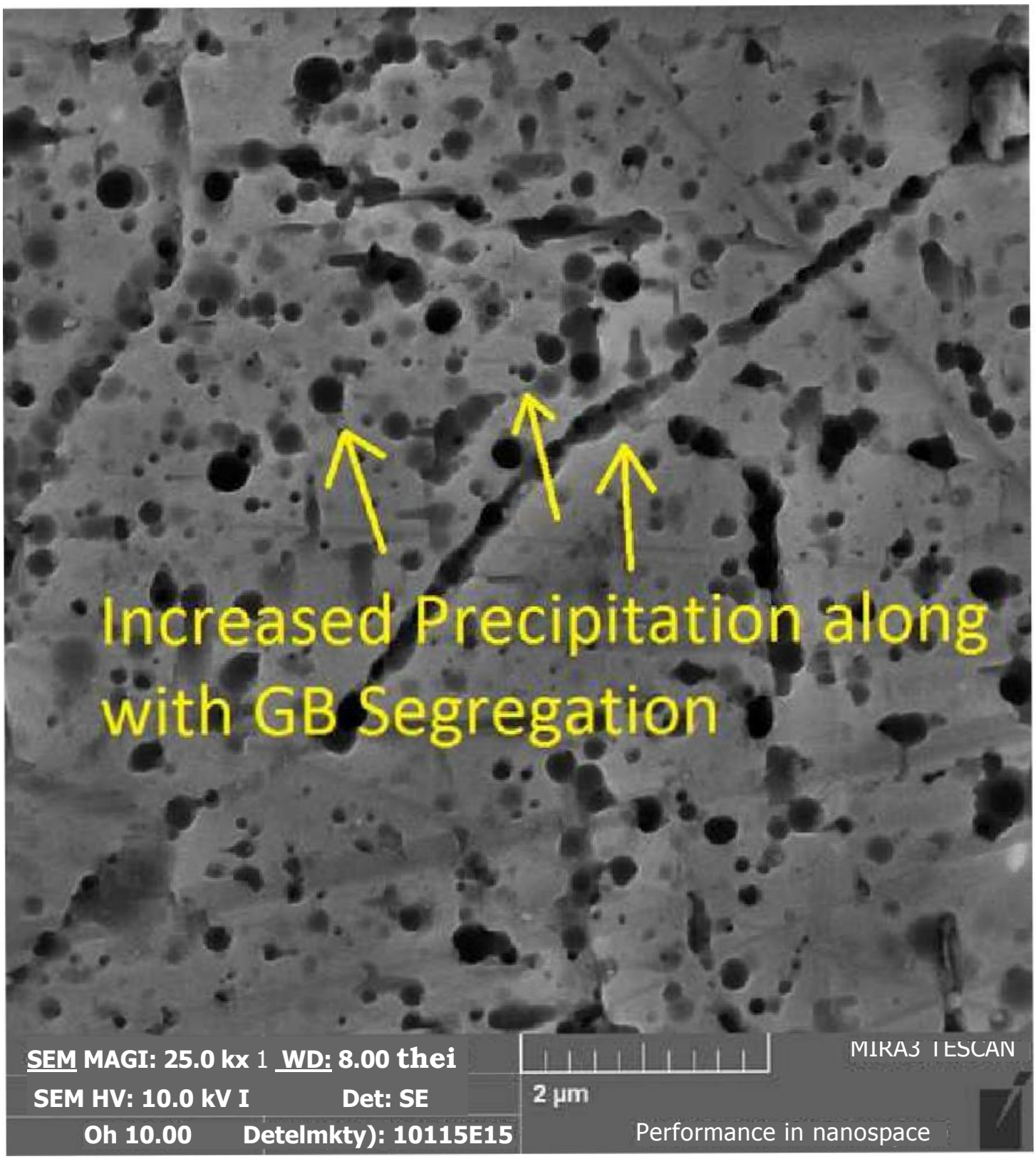
Increased Precipitation along with GB Segregation
SEM MAGI: 25.0 kx 1 WD: 8.00 thei
SEM HV: 10.0 kV I Det: SE
Oh 10.00 Detelmkty): 10115E15
2 µm
MIRA3 TESCAN
Performance in nanospace

Figure 15

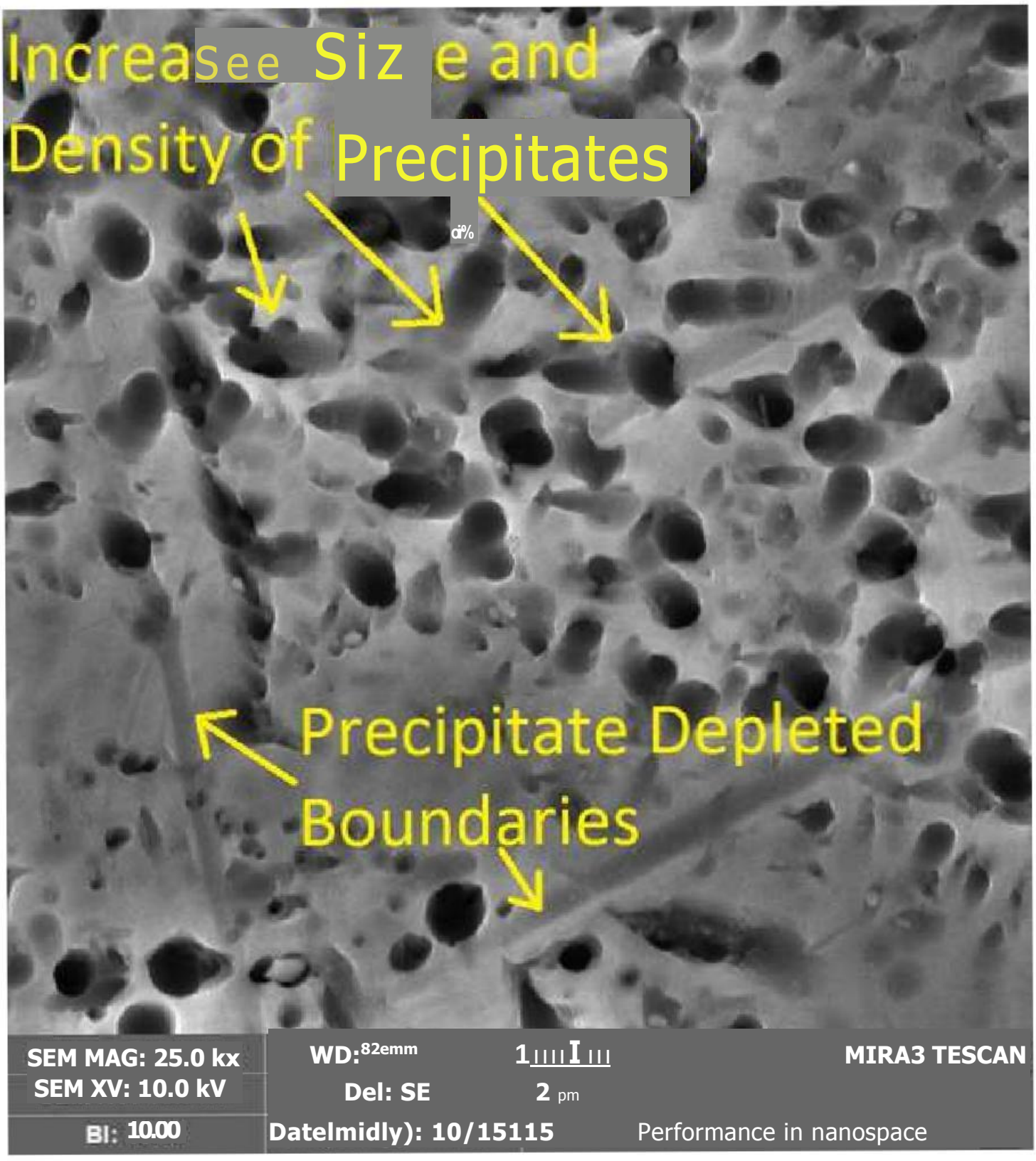
Increasee Siz e and
Density of Precipitates
Precipitate Depleted
Boundaries
SEM MAG: 25.0 kx
SEM XV: 10.0 kV
BI: 10.00
WD: 82emm
Del: SE
Datelmidly): 10/15115
2 pm
MIRA3 TESCAN
Performance in nanospace